

Eavesdropper Performance in Cellular CDMA (1)

ANDREW MCKELLIPS, SERGIO VERDÚ

Department of Electrical Engineering, Princeton University, Princeton, NJ 08544
andyman@EE.Princeton.EDU

Abstract. We study eavesdropper performance in power-controlled cellular CDMA systems. A significant hindrance to eavesdropping in the reverse channel is the wide range of potential received powers from active users; although power control insures that all users are received with approximately equal power at the base station, it does not concern itself with the rest of the cell. Susceptibility to the near-far problem is demonstrated, and performance sensitivity to eavesdropper location is shown to depend on a single off-centered-ness parameter. Both circular and linear cell geometries are considered, with log-distance and log-normal shadowing models adopted for signal path loss. A comparison of several eavesdropper detection strategies is performed, demonstrating a potential for significant performance improvement through the use of multiuser detection techniques.

1. INTRODUCTION

In this paper, we are interested in assessing achievable performance for an eavesdropper located at an arbitrary position in a cellular communication system which employs power control. The results form a performance guideline for eavesdropping agencies which operate subject to various location considerations, and which are either employing or considering employment of various receiver structures. The potential for performance improvement through the use of multiuser detection techniques designed to mitigate multiple-access interference is analyzed. From the point of view of cellular system evaluation and improvement, specifically in terms of eavesdropping susceptibility, the results represent a fair assessment of potential performance for an eavesdropper employing multiuser detection techniques.

Power control is implemented in cellular communication systems to insure that active users are received with approximately equal power at the base station. The purpose of such control is to mitigate multiple-access interference in the reverse channel by preventing the domination of any user's signal by that of any other user at the base station detector, effectively realizing a fair distribution of MAI among all users. The potential for a significant discrepancy in received user power is com-

monly referred to as the near-far problem, and can result in significant performance degradation.

The form and extent of power control implementation can vary according to the types of power loss encountered by signals during propagation. In a predominantly line-of-sight system, signal path loss is primarily dependent on the separation between the user and base station, and hence power control can be effectively realized in simple open loop fashion by mandating that each user estimate encountered signal power attenuation as a function of received signal power from the base station and adjust its transmit power accordingly. In systems subject to fast fading effects such as multipath, a closed loop feedback control implementation is necessary to counteract unpredictable dynamic signal attenuation; given a fast enough control loop sampling rate, users' received powers are kept within a reasonable proximity to the prescribed reference level at the base station [1]. Closed loop power control based on measurements of signal-to-interference-and-noise ratio (*SINR*) has been considered as a viable alternative to control based on direct measurements of absolute received power, motivated by easier implementation and a stronger tie to performance criteria, but involving stability issues as a result of the interdependencies between users' *SINRs* and signal strengths [2].

Common to all forms of power control is the mitigation of received power at the base station with disregard to the induced power distribution throughout the rest of the communication cell. Consequently, an eavesdropper located somewhere other than the base station may not

(1) This work was supported in part by the U.S. Army Research Office under Grant DAAH04-96-1-0379.

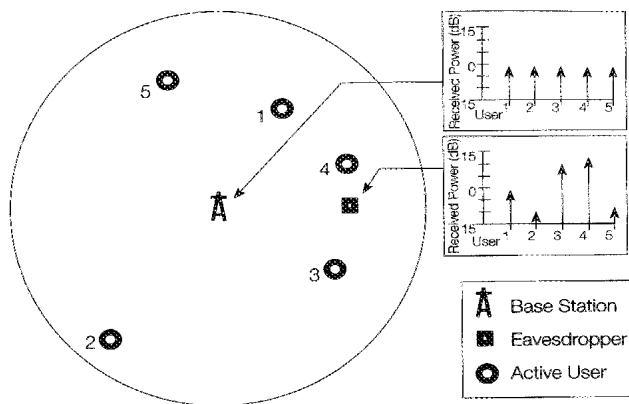


Fig. 1 - Near-far effect for an eavesdropper in a power-controlled cell.

benefit from power control, and is susceptible to near-far effects as a result. Consider for example the situation depicted in Fig. 1, where an eavesdropper is attempting to detect the transmission of user 1 amidst strong interference from other active users; given an unfavorable distribution of users and a strong enough cross-correlation between users' signals, such detection will be rendered impossible using conventional detection techniques. In this paper, we study the performance of an eavesdropper located at an arbitrary position within a CDMA cell. In section 2, we compute the distribution of received power throughout a communication cell with ideal power control for both standard circular cell and linear cell geometries. We then compare several eavesdropper detection strategies in section 3. Section 4 considers the effect of shadowing on eavesdropper performance. Our conclusions are presented in section 5.

2. RECEIVED POWER DISTRIBUTION

2.1. Circular cell geometry

Consider a circular communication cell of radius A , with a single centrally-located base station, K active users, and an eavesdropper located a distance $a \leq A$ from the base station. The locations of the users within the cell are modelled as uniformly random and independent. Path loss is assumed to satisfy a log-distance law of the form

$$p_R = p_T/d^{2\alpha} \tag{1}$$

where p_T represents the user's transmit power, p_R the received power, d the propagation distance, and 2α the path loss exponent, with α typically ranging from 1 (rural) to 2 (urban). The numerical substitution $\alpha = 1$ is made throughout unless otherwise noted; in light of the observation that the range of potential received powers increases with α , the choice $\alpha = 1$ represents a best-case scenario on the part of the eavesdropper, and a lower bound on the performance-improving potential of multi-

user detection techniques. The additional effect of log-normal shadowing will be considered in section 4.

It is interesting to note that the range of potential received powers from active users throughout the cell at an off-center eavesdropper can actually increase as a result of base station power control. To see this, consider an eavesdropper located at the edge of the cell and a pair of active users. Without power control (in which case the users transmit with equal constant power p_T), the maximum ratio of received powers is achieved when one user is situated close enough to the eavesdropper to be received with approximate power p_T (assuming without loss of generality unit eavesdropper antenna gain) while the other is situated across the cell at a distance $2A$ from the eavesdropper; in this case, the received power ratio is $(2A)^{2\alpha}$ according to (1). With power control, the maximum received power is achieved by displacing the distant user to a position close enough to the base station where it need only transmit with approximately the reference power p_0 (assuming again without loss of generality unit base station antenna gain). Such a user will be received with approximate power $p_0/A^{2\alpha}$ at the eavesdropper. Meanwhile, the user located near the eavesdropper needs to transmit with power $p_0A^{2\alpha}$ according to (1), and thus the ratio of received powers at the eavesdropper is equal to $A^{4\alpha}$, which can clearly be significantly greater than the maximum received power ratio $(2A)^{2\alpha}$ without employed power control for cells with relatively large radius, rendering power control a potential contributor to the eavesdropper near-far problem.

For an active user located in the far-field region of the base station and eavesdropper antennas at a distance u from the base station ($0 < u \leq A$) and on a line θ radians from the line between eavesdropper and base station (Fig. 2), the received power at the eavesdropper is given by

$$p = [u^2/(u^2 + a^2 - 2ua \cos \theta)]^\alpha \tag{2}$$

where the reference level at the base station is taken to be 0 dB. Fig. 2 depicts a representative set of contours corresponding to equal received power at the eavesdropper. In this paper we find the resulting cumulative distribution function (CDF) of the random variable P

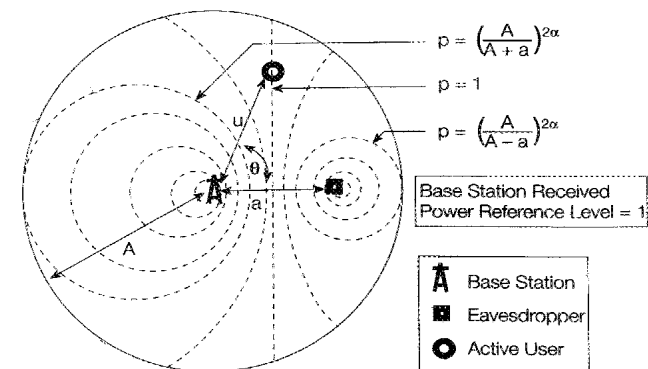


Fig. 2 - Equal received power contours for an eavesdropper.

representing received power from a user distributed uniformly within the cell:

of received power increased as the eavesdropper moves away from the base station.

$$F_p(p) = \begin{cases} 0, & 0 \leq p < \frac{1}{M} \\ \frac{p^{1/\alpha} \gamma^2}{(1-p^{1/\alpha})^2}, & \frac{1}{M} \leq p \leq \max \left[\frac{1}{M}, \frac{1}{(1+\gamma)^{2\alpha}} \right] \\ \frac{1}{2} + \frac{1}{\pi} \sin^{-1} \left[\frac{p^{1/\alpha} (1+\gamma^2) - 1}{2 p^{1/\alpha} \gamma} \right] + \frac{p^{1/\alpha} \gamma^2}{(1-p^{1/\alpha})^2} \left\{ \frac{1}{2} - \frac{1}{\pi} \sin^{-1} \left[\frac{p^{1/\alpha} (p^{1/\alpha} + 1) \gamma^2 - (1-p^{1/\alpha})^2}{2 p^{3(2\alpha)} \gamma^2} \right] \right\} + \\ \frac{\sqrt{2 p^{1/\alpha} (1+\gamma^2) - p^{2/\alpha} (1-\gamma^2)^2 - 1}}{2 \pi (p^{1/\alpha} - 1)}, & \max \left[\frac{1}{M}, \frac{1}{(1+\gamma)^{2\alpha}} \right] < p < 1 \\ \frac{1}{2} + \frac{1}{\pi} \sin^{-1} \left(\frac{\gamma}{2} \right) + \frac{\gamma}{4 \pi} \sqrt{4 - \gamma^2}, & p = 1 \\ \frac{1}{2} + \frac{1}{\pi} \sin^{-1} \left[\frac{p^{1/\alpha} (1+\gamma^2) - 1}{2 p^{1/\alpha} \gamma} \right] - \frac{p^{1/\alpha} \gamma^2}{(1-p^{1/\alpha})^2} \left\{ \frac{1}{2} - \frac{1}{\pi} \sin^{-1} \left[\frac{p^{1/\alpha} (p^{1/\alpha} + 1) \gamma^2 - (1-p^{1/\alpha})^2}{2 p^{3(2\alpha)} \gamma^2} \right] \right\} + \\ \frac{\sqrt{2 p^{1/\alpha} (1+\gamma^2) - p^{2/\alpha} (1-\gamma^2)^2 - 1}}{2 \pi (p^{1/\alpha} - 1)}, & 1 < p < \min \left[M, \frac{1}{(1-\gamma)^{2\alpha}} \right] \\ 1 - \frac{p^{1/\alpha} \gamma^2}{(1-p^{1/\alpha})^2}, & \min \left[M, \frac{1}{(1-\gamma)^{2\alpha}} \right] \leq p \leq M \\ 1, & p > M \end{cases} \quad (3)$$

where $\gamma = a/A$ and the range of $\sin^{-1}(\cdot)$ is taken to be $[-\pi/2, \pi/2]$. The restriction of potential received power to the interval $[1/M, M]$ represents the inconsistency of the path loss-model (1) for small transmitter-receiver separation d . Of note is the dependency of the received power distribution on the location of the eavesdropper and the radius of the cell through a single parameter $0 \leq \gamma \leq 1$ representing "off-centered-ness" of the eavesdropper. Fig. 3 depicts $F_p(p)$ for several values of eavesdropper off-centered-ness γ . As expected, the variance

Consider a two-user system with an eavesdropper interested in detecting the signal of user 1, who is received with power p_1 . If we assume that the eavesdropper uses a conventional matched-filter detector and prescribe a required signal-to-interference (SIR) threshold Γ below which the eavesdropper can not operate satisfactorily, with interference power from user 2 given by τp_2 , we can write the probability of eavesdropper outage as

$$P(\text{outage}) = 1 - F(p_1/\tau\Gamma)$$

For a relatively large number of independently located users K , we can approximate the sum of received powers from interfering users 2 through K with a Gaussian distribution with mean $(K - 1) E(P)$ and variance $(K - 1) [E(P^2) - E(P)^2]$, where $E(P)$ and $E(P^2)$ are expected values and are obtained through (3). If we assume that interference is proportional to total received power from interfering users, then probability of eavesdropper outage is in this case given by

$$P(\text{outage}) = Q \left\{ \frac{p_1/\tau\Gamma - (K - 1) E(P)}{\sqrt{(K - 1) [E(P^2) - E(P)^2]}} \right\}$$

where $Q(\cdot)$ represents the tail of the standard unit-variance Gaussian distribution. Fig. 4 depicts eavesdropper

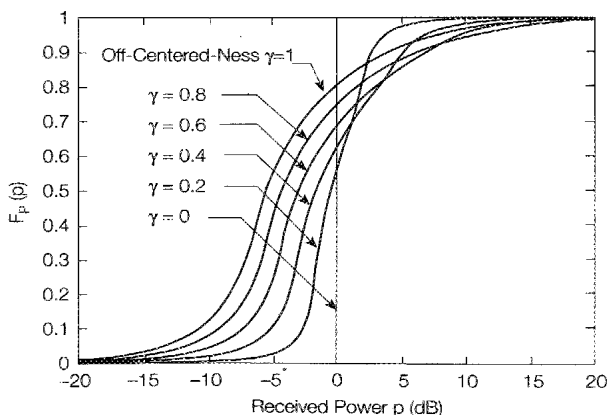


Fig. 3 - CDF of received power at various off-center locations for a uniformly-distributed power-controlled active user in a circular cell.

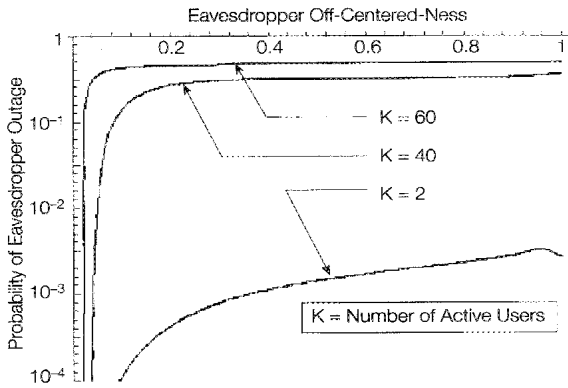


Fig. 4 - Eavesdropper outage probability with mean desired user received power.

outage probabilities as a function of off-centered-ness for a cell with different loads for $p_1 = E(P)$, $\Gamma = 3$ dB, $\tau = 1/128$ and $M = 30$ dB. It is clear from the figure that eavesdropper performance is highly sensitive to off-centered-ness, motivating the investigation of alternative eavesdropper detection strategies designed to suppress interference in the following section.

2.2. Linear cell geometry

In light of the complexity of the eavesdropper received power distribution (3) for a uniformly distributed active user in a circular cell, we consider a simpler linear cell geometry in order to develop further results and insight. The linear CDMA cell depicted in Fig. 5 exhibits many of the properties of interest to an eavesdropper situated in a circular cell, in particular a location-dependent induced distribution of received power from active users even under ideal power control, and hence susceptibility to the near-far problem. Such a cell configuration is of practical interest as well, for instance in the analysis of calls generated by freeway traffic during rush hour.

In the linear cell model, active users are located on a straight line segment of length $2A$, with a centrally-located base station employing perfect power control. Under the signal propagation model 1, the induced CDF of received power at an eavesdropper located a units from the base station from a uniformly distributed active user is given by

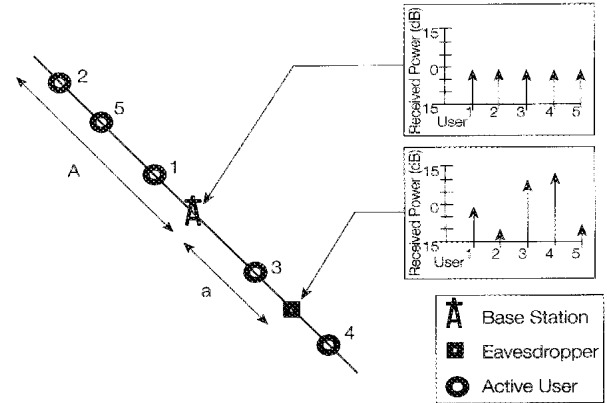


Fig. 5 - Linear cell geometry.

where $\gamma = a/A$. Fig. 6 depicts received power CDFs for several values of eavesdropper off-centered-ness γ . The variance of received power is seen to increase as the eavesdropper-to-base-station separation grows for the linear cell model as well.

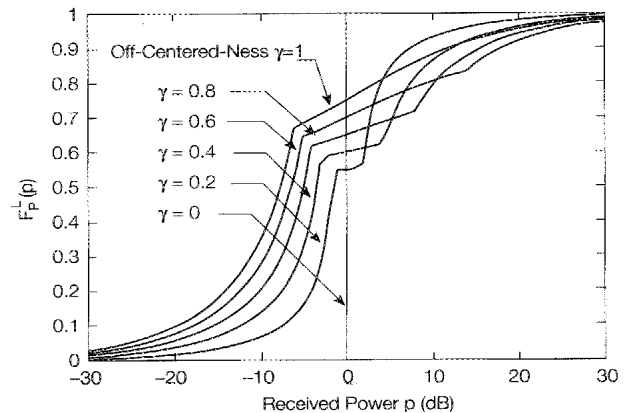


Fig. 6 - CDF of received power at various off-center locations for a uniformly-distributed power-controlled active user in a linear cell.

3. TWO-USER CDMA SYSTEM ANALYSIS

We focus attention on a two-user CDMA system, facilitating a detailed analysis of some of the major issues confronting an eavesdropper. Consider a CDMA

$$F_p^L(p) = \begin{cases} 0, & 0 \leq p < \frac{1}{M} \\ \frac{p^{1/2\alpha} \gamma}{1 - p^{1/\alpha}}, & \frac{1}{M} \leq p \leq \max \left[\frac{1}{M}, \frac{1}{(1 + \gamma)^{2\alpha}} \right] \\ \frac{1}{2} + \frac{p^{1/2\alpha} \gamma}{2(1 + p^{1/2\alpha})}, & \max \left[\frac{1}{M}, \frac{1}{(1 + \gamma)^{2\alpha}} \right] < p < \min \left[M, \frac{1}{(1 - \gamma)^{2\alpha}} \right] \\ 1 - \frac{p^{1/2\alpha} \gamma}{p^{1/\alpha - 1}}, & \min \left[M, \frac{1}{(1 - \gamma)^{2\alpha}} \right] \leq p \leq M \\ 1, & p > M \end{cases} \tag{4}$$

system with two active users, where users 1 and 2 are assigned the signature waveforms $s_1(t)$ and $s_2(t)$ respectively. The waveforms are assumed to be time-limited to the interval $[0, T]$ where T is the inverse of the bit transmission rate, and are assumed to exhibit normalized signal energy $\int_0^T s_1^2(t) dt = \int_0^T s_2^2(t) dt = 1$. User 1 transmits the information-bearing signal

$$u_1(t) = \sum_{i=-\infty}^{\infty} A_{1,i} b_{1,i} s_1(t - iT)$$

and user 2 the signal

$$u_2(t) = \sum_{i=-\infty}^{\infty} A_{2,i} b_{2,i} s_2(t - iT)$$

where the $b_{1,i}$ and $b_{2,i}$ are all independent and identically distributed, taking on the values $+1$ and -1 equiprobably, and the transmitted amplitudes $A_{1,i}$ and $A_{2,i}$ are chosen to realize ideal power control at the base station. We assume that the active users transmit synchronously, simplifying the analysis considerably while providing a good characterization of performance behavior in the asynchronous case. In the synchronous case, base station and eavesdropper performance both hinge strongly on the cross-correlation

$$\rho = \int_0^T s_1(t) s_2(t) dt$$

between the two users' signature waveforms. Our goal is to analyze eavesdropper performance as it depends on ρ and off-centered-ness γ .

3.1. Eavesdropper detection strategies

According to the described model, the eavesdropper is faced with determining the information-bearing bits $\{b_{1,i}\}$ from user 1 given the reception

$$y(t) = \sum_{i=-\infty}^{\infty} \left[\sqrt{p_{1,i}} b_{1,i} s_1(t - iT) + \sqrt{p_{2,i}} b_{2,i} s_2(t - iT) \right] + n(t)$$

where $n(t)$ is white Gaussian background noise with variance σ^2 and $p_{1,i}$ and $p_{2,i}$ are received powers at the eavesdropper, given by (2). In the synchronous case, the eavesdropper need only perform bit-by-bit detection, since all information concerning the reception of any given bit is contained within the corresponding signaling interval. Focusing on the detection of the bit transmitted by user 1 at time 0, the eavesdropper must determine b_1 from the reception

$$y(t) = \sqrt{p_1} b_1 s_1(t) + \sqrt{p_2} b_2 s_2(t) + n(t) \quad (5)$$

where for the sake of clarity we have suppressed nota-

tion associated with the full transmission sequence. When both users are independently and uniformly distributed within the cell, p_1 and p_2 will take on independent and identical distributions according to (3) for a circular cell geometry and (4) for a linear geometry. Note that the corresponding received signal at the base station is given by

$$y_{BS}(t) = b_1 s_1(t) + b_2 s_2(t) + n_{BS}(t)$$

under ideal power control, where $n_{BS}(t)$ is white Gaussian background noise.

We will assume throughout that the eavesdropper has access to the signature waveforms and is synchronized with the rest of the system. We discuss the potential operation of an eavesdropper without such information at the end of this section. One eavesdropper strategy which immediately comes to mind is the conventional matched-filter detector, which yields the decision

$$\hat{b}_1(\text{conv}) = \text{sgn} \left[\int_0^T y(t) s_1(t) dt \right]$$

where $\text{sgn}(x)$ takes the value 1 if $x \geq 0$ and -1 if $x < 0$. The probability of detection or error is given by

$$P_e(\text{conv}) = \frac{1}{2} \left[Q \left(\frac{\sqrt{p_1} - \rho \sqrt{p_2}}{\sigma} \right) + Q \left(\frac{\sqrt{p_1} + \rho \sqrt{p_2}}{\sigma} \right) \right]$$

from which it is clear that the conventional detector will perform satisfactorily as long as the background noise power remains small and $\rho^2 p_2 \ll p_1$. In light of the analysis of the previous section, where it was shown that an off-centered eavesdropper is susceptible to the near-far problem (characterized by $p_2 \gg p_1$), the conventional detector may not provide dependable results.

Hence, it is of interest to an eavesdropper to consider using alternative detection strategies, especially those designed to mitigate MAI. Given knowledge of the signature waveforms and received powers of all K active users, optimum detection amounts to performing a maximum likelihood decision over all possible 2^K potential transmitted bit combinations. In the two-user case, jointly optimum detection of user 1 is achieved by computing (e.g. [3])

$$y_1 = \int_0^T y(t) s_1(t) dt$$

as in the conventional detector, and in addition

$$y_2 = \int_0^T y(t) s_2(t) dt$$

leading to the decision

$$\hat{b}_1(\text{opt}) = \begin{cases} \text{sgn}[y_1], & \min(\sqrt{p_1}|y_1|, \sqrt{p_2}|y_2|) \geq |\rho|\sqrt{p_1 p_2} \\ \text{sgn}[y_1 - \text{sgn}(\rho)y_2], & \text{otherwise} \end{cases}$$

A drawback to optimum detection is the exponential growth in complexity with an increasing number of active users. An alternative strategy with linear complexity is the decorrelating detector [4], which also requires knowledge of the signature waveforms of all users, but not the received powers. The decorrelating detector eliminates all MAI, but at the expense of increased background noise power, and in the two-user case amounts to deciding

$$\hat{b}_1(\text{dec}) = \text{sgn}(y_1 - \rho y_2)$$

Another alternative is the Minimum Mean Square Error (MMSE) linear multiuser detector [5, 6, 7, 8, 9] which minimizes the sum of MAI power and background noise power. Although the MMSE detector requires knowledge of the signature waveforms and received powers of all users, in addition to the background noise power, it lends itself to a blind adaptive implementation [10]. When the eavesdropper does not have access to the desired user's signature waveform in a system which assigns pseudo-random signature sequences, there is the potential to invoke subspace techniques in order to employ the blind version of the MMSE receiver [11]. In the two-user system, the MMSE decision is given by

$$\hat{b}_1(\text{MMSE}) = \text{sgn}\left[\left(1 + \frac{\sigma^2}{p_2}\right)y_1 - \rho y_2\right]$$

As is apparent from the discussion above, varying degrees of information regarding the users' signature waveforms, received amplitudes and background noise power are required for implementation of the various receivers considered in this section. Much recent work has focused on the development of techniques to either gather such information, or to recover users' information bit streams, when the relevant quantities are not directly accessible at the receiver. For instance, it is possible to recover the bit streams of all users without knowledge of any signature waveforms [11], although the channel characteristics of all users must remain constant and prohibitive complexity is reported in [11]. A significant performance improvement and reduction in complexity is achievable given knowledge of the desired user's waveform, with adaptive techniques presented in [10, 12]. To remain within the scope of this study, we will assume that the receiver of interest has access to the relevant quantities, noting that the corresponding analysis represents a best-case performance characterization from the point of view of the eavesdropper.

3.2. Eavesdropper detection strategy comparison

In order to compare eavesdropper detection strategies, we apply the performance criteria of asymptotic

multiuser efficiency (AME) and bit error rate (BER). The AME quantifies the SNR attenuation required in an equivalent single-user system (without interferers) in order to match error performance with the given multiuser system in the low background noise region. The following expressions quantify the two-user AMEs of the conventional, optimal, decorrelating and linear MMSE detectors respectively for given received powers p_1 and p_2 from users 1 and 2 respectively, and for a given cross-correlation ρ [3]:

$$\eta(\text{conv}; r, \rho) = \max^2\left(0, 1 - |\rho|\sqrt{p_2/p_1}\right) \tag{6}$$

$$\eta(\text{opt}; r, \rho) = \min\left(1, 1 + p_2/p_1 + 2|\rho|\sqrt{p_2/p_1}\right)$$

$$\eta(\text{dec}; r, \rho) = 1 - \rho^2 \tag{7}$$

$$\eta(\text{MMSE}; r, \rho) = 1 - \rho^2$$

Note that the AMEs of the decorrelating and linear MMSE detectors are equal and are independent of the received powers. In addition, the AME of the conventional and optimal detectors depend on p_1 and p_2 through the ratio $r = p_2/p_1$ only, making this quantity of particular interest in the analysis of eavesdropper performance. Hence, we turn attention to characterizing the induced distribution of received power ratio $R = P_2/P_1$ for two independently and uniformly distributed users, given by

$$F_R = \int_0^\infty F_p(rp) dF_p(p) \tag{8}$$

where F_p is the CDF of received power. While closed-form evaluation of F_R is apparently infeasible for a circular cell geometry, we obtain for a linear cell geometry the expression

$$F_R^L(r) = \begin{cases} 0, & 0 \leq r < \frac{1}{M^2} \\ 1 - \Psi_1(r^{-1/2\alpha}), & \frac{1}{M^2} \leq r \leq \max\left[\frac{1}{M^2}, \left(\frac{1-\gamma}{1+\gamma}\right)^{2\alpha}\right] \\ 1 - \Psi_2(r^{-1/2\alpha}), & \max\left[\frac{1}{M^2}, \left(\frac{1-\gamma}{1+\gamma}\right)^{2\alpha}\right] < r < 1 \\ \frac{1}{2}, & r = 1 \\ \Psi_2(r^{1/2\alpha}), & 1 < r < \min\left[M^2, \left(\frac{1+\gamma}{1-\gamma}\right)^{2\alpha}\right] \\ \Psi_1(r^{1/2\alpha}), & \min\left[M^2, \left(\frac{1+\gamma}{1-\gamma}\right)^{2\alpha}\right] \leq r \leq M^2 \\ 1, & r > M^2 \end{cases} \tag{9}$$

where

the desired user was assumed to be received with mean

$$\Psi_1(x) = \frac{x^2 + x\gamma(\gamma-2) - 1}{x^2 - 1} + \frac{\gamma^2 x}{4(x+1)^2} \log \left\{ \frac{(x-\gamma-1)[x(1-\gamma)-1]}{(x+\gamma+1)[x(1+\gamma)-1]} \right\} + \frac{\gamma^2 x}{4(x-1)^2} \log \left\{ \frac{(x+\gamma+1)[x(1-\gamma)+1]}{(x-\gamma+1)[x(1+\gamma)+1]} \right\} + \frac{\gamma^2 x(x^2+1)}{2(x^2-1)^2} \log \left\{ \frac{[x(1+\gamma)+1][x(1+\gamma)-1](x-\gamma+1)(x+\gamma-1)}{x^2(x+\gamma+1)(x-\gamma-1)[x(1-\gamma)+1][x(1-\gamma)-1]} \right\}$$

$$\Psi_2(x) = \frac{x^2(\gamma+3) + 2x\gamma(2\gamma-3) + \gamma - 3}{4(x^2-1)} + \frac{\gamma^2 x}{4(x+1)^2} \log \left\{ \frac{\gamma^2 x}{[x(1+\gamma)-1](x+\gamma-1)} \right\} + \frac{\gamma^2 x}{4(x-1)^2} \log \left\{ \frac{(x+\gamma+1)[x(1-\gamma)+1]}{(x-\gamma+1)[x(1+\gamma)+1]} \right\} + \frac{\gamma^2 x(x^2+1)}{2(x^2-1)^2} \log \left\{ \frac{[x(1+\gamma)+1][x(1+\gamma)-1](x-\gamma+1)(x+\gamma-1)}{x^2 \gamma^2 (x+\gamma+1)[x(1-\gamma)+1]} \right\}$$

for the CDF of received power ratio P_2/P_1 via (4). Fig. 7 depicts F_R^L for two values of eavesdropper off-centeredness, along with a log-normal approximation with zero mean and variance determined via (4). Computation demonstrates a good fit between F_R^L and a log-normal approximation, especially for off-centeredness values $\gamma \geq 0.1$, and hence we apply a log-normal approximation for the CDF F_R of received power ratio for a circular cell geometry, which has been demonstrated through simulation to provide accurate performance results.

Given the eq. (9) for F_R^L , we can extend our analysis of eavesdropper outage probabilities of section 2, where

power, to the more general case where both the desired and interfering users are independently and uniformly distributed within a linear cell. Fig. 8 depicts outage probabilities for a linear cell as a function of eavesdropper off-centeredness for a SIR threshold of $\Gamma = 3$ dB and interference-to-received-power factor $\tau = 1/128$. Curves are computed using a log-normal approximation to F_R^L as well for comparison, demonstrating good relative accuracy for $\gamma \geq 0.1$.

We now turn attention to evaluating expected eavesdropper AME for the two-user cell under consideration; although the expected value of AME does not constitute a full statistical performance description, it represents the primary quantity of interest to which we restrict attention in this study. Applying the log-normal approximation to received power ratio with mean 0 dB and standard deviation σ_R given (in dB) through (3) by

$$\sigma_R^2 = 2E [(10 \log_{10} P)^2] - 2E [10 \log_{10} P]^2 \tag{10}$$

The expected AMEs of the conventional and optimal detectors for two uniformly distributed users with cross-correlation ρ are then given by

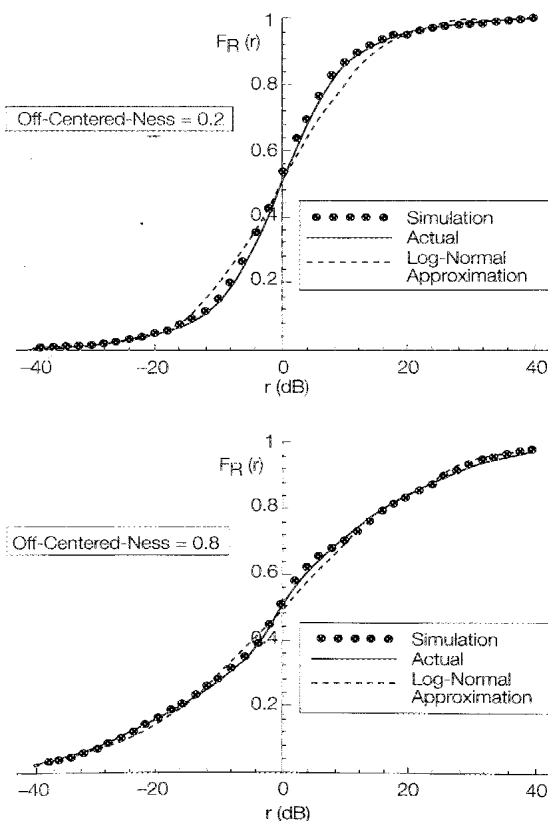


Fig. 7 - CDF of received power ratio for two uniformly-distributed users.

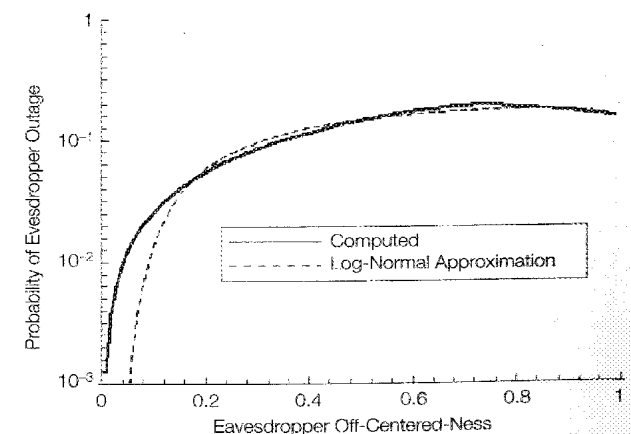


Fig. 8 - Eavesdropper outage probability for two uniformly-distributed users.

$$E[\eta(\text{conv}; R, \rho)] = \frac{20}{\sqrt{2\pi\sigma_R^2 \log(10)}} \int_0^{1/|\rho|} \frac{(1-|\rho|\tau)^2}{\tau} \exp\left[-\frac{(20 \log_{10} \tau)^2}{2\sigma_R^2}\right] d\tau \quad (11)$$

$$E[\eta(\text{opt}; R, \rho)] = \frac{20}{\sqrt{2\pi\sigma_R^2 \log(10)}} \int_0^{2/|\rho|} \frac{1+\tau^2-2|\rho|\tau}{\tau} \exp\left[-\frac{(20 \log_{10} \tau)^2}{2\sigma_R^2}\right] d\tau + Q\left[\frac{20 \log_{10}(2|\rho|)}{\sigma_R}\right] \quad (12)$$

where $\log(\cdot)$ denotes the natural logarithm. Fig. 9 depicts expected eavesdropper performance using various detection strategies for two uniformly and independently located users with signal cross-correlation $\rho = 0.2$ as a function of eavesdropper off-centered-ness. The curves are computed using the log-normal approximation to received power ratio via (11) and (12); simulation results are shown for comparison. Similar curves are depicted in Fig. 10 for a cross-correlation value of 0.8. Of note is the increased overall discrepancy between detector performances for the higher cross-correlation value, an expected benefit of the interference-mitigating multiuser detectors. The apparent improvement in conventional detector performance in Fig. 10 as the eavesdropper moves away from the base station can be explained by the nonlinearity in the AME eq. (6) at $r = 0$. A similar behavior is exhibited by the optimal detector in Fig. 10, and can be explained by the quadratic nature of (7).

While AME is an effective measure of detector performance for arbitrarily low noise power, actual system performance will also be affected by detector performance sensitivity to background noise. In order to evaluate eavesdropper performance for non-negligible noise power levels, Figs. 11 and 12 depict BER curves for the two-user

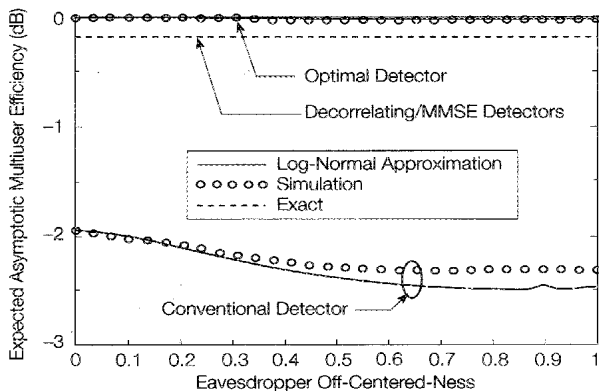


Fig. 9 - Asymptotic multiuser efficiency for various detection strategies (two uniformly-distributed users with cross-correlation $\rho = 0.2$).

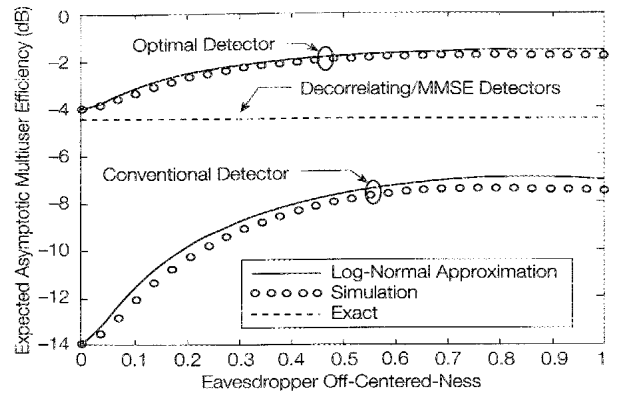


Fig. 10 - Asymptotic multiuser efficiency for various detection strategies (two uniformly-distributed users with cross-correlation $\rho = 0.8$).

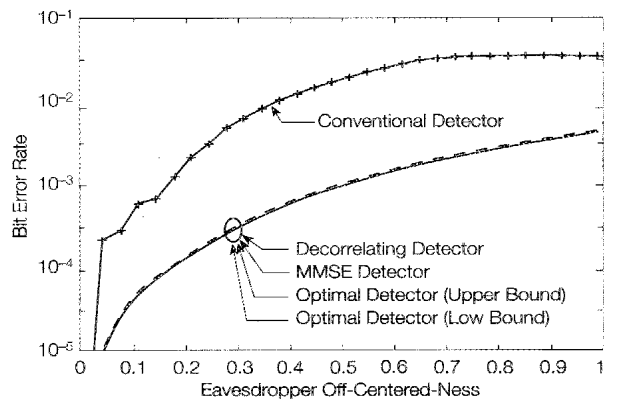


Fig. 11 - Bit Error Rate for various detection strategies, $SNR = 20$ dB (two uniformly-distributed users with cross-correlation $\rho = 0.2$).

system described above at a SNR level of 20 dB, as obtained through simulation of the users' locations using exact BER expressions. System SNR is taken to be the ratio of signal power from a single active user to background noise power for an eavesdropper situated at the base station. Figs. 13 and 14 depict similar curves for an SNR level of 10 dB. It is clear that BER performance is improved significantly in all cases through the use of multiuser detection. It is also apparent that for relatively low cross-corre-

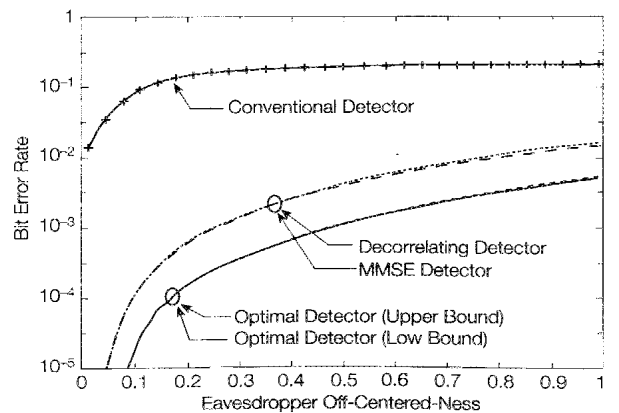


Fig. 12 - Bit Error Rate for various detection strategies, $SNR = 20$ dB (two uniformly-distributed users with cross-correlation $\rho = 0.8$).

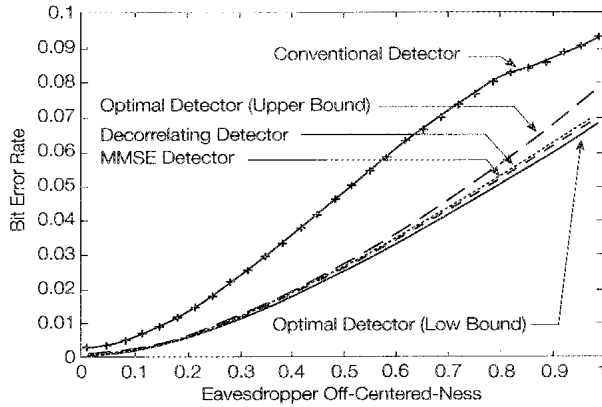


Fig. 13 - Bit Error Rate for various detection strategies, SNR = 10 dB (two uniformly-distributed users with cross-correlation $\rho = 0.2$).

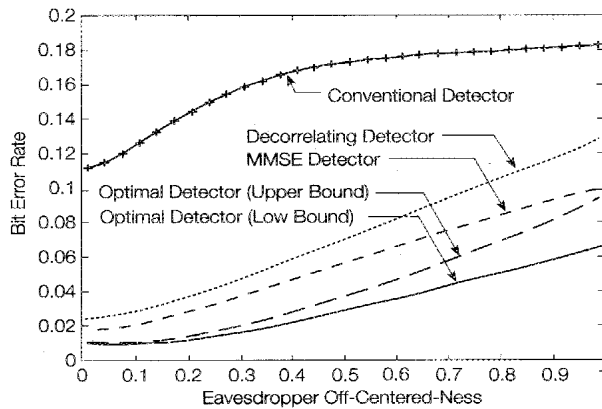


Fig. 14 - Bit Error Rate for various detection strategies, SNR = 10 dB (two uniformly-distributed users with cross-correlation $\rho = 0.8$).

lation values; the loss in performance incurred through use of the lower-complexity decorrelating and MMSE detectors is very small in comparison to optimal detection.

4. SHADOWING

The log-distance path loss model we have adopted to this point can be augmented to incorporate the effects of shadowing, which models unpredictable signal attenuation due to varying terrain and obstructions within the cell. Typically, shadowing is modelled by a log-normal random variable [13] with variance σ_s^2 derived from system measurements. The log-distance model (1) is thus augmented to the new path loss expression

$$P_R = X P_T / d^{2\alpha} \tag{13}$$

where X is a log-normal random variable representing shadowing effects, $10 \log_{10} X \sim N(0, \sigma_s^2)$. We assume that the base station and eavesdropper experience independent shadowing from different users and from each other, which is reasonable for non-negligible eavesdropper off-centered-ness and inter-user separation.

If the base station compensates for shadowing through the use of feedback power control, an achievable goal given the typically slow behavior of shadowing dynamics in comparison with transmission bit rates, received power p^S is given by

$$p^S = \frac{X^e}{X^{bs}} p \tag{14}$$

where p is received power for log-distance path loss, given by (2), and X^e and X^{bs} represent shadowing experienced by the base station and eavesdropper respectively. Without shadowing compensation at the base station, received power is given by

$$p^S = X^e p$$

We will use the model (14) under the assumption that the base station maintains ideal power control even in the presence of shadowing. Of interest is the fact that power control amplifies the deleterious effect of shadowing at the eavesdropper. To see this, note that received power is given in dB under ideal power control by

$$10 \log_{10} p^S = 10 \log_{10} X^e - 10 \log_{10} X^{bs} + 10 \log_{10} p$$

and in the absence of base station compensation by

$$10 \log_{10} p^S = 10 \log_{10} X^e + 10 \log_{10} p$$

Since $10 \log_{10} X^e$ and $10 \log_{10} X^{bs}$ are independent normal random variables, the variance of received power distribution in the case of ideal power control is double that without compensation; coupled with the observation from section 2 that power control contributes to the near-far problem for the eavesdropper by introducing a larger potential range of received powers, we conclude that employed power control is a significant hindrance to the eavesdropper.

Recalling the two-user analysis of the previous section, where the ratio of received powers P_2/P_1 at an eavesdropper for two uniformly and independently located active users under a log-distance path loss model was found to be well-approximated by a log-normal random variable, we note that the ratio (in dB) of received powers P_2^S/P_1^S in the added presence of shadowing effects can be rewritten according to (14) as

$$10 \log_{10} (P_2^S/P_1^S) = 10 \log_{10} X_2^e - 10 \log_{10} X_1^e -$$

$$10 \log_{10} X_2^{bs} + 10 \log_{10} X_1^{bs} + 10 \log_{10} (P_2/P_1)$$

where the terms in the summation are mutually independent zero-mean normal random variables, with X_1^e , X_2^e , X_1^{bs} and X_2^{bs} exhibiting variance σ_s^2 , and the log-distance power ratio $10 \log_{10} (P_2/P_1)$ exhibiting variance σ_R^2 according to (10). Hence, given the log-normal approximation for received power ratio under the log-

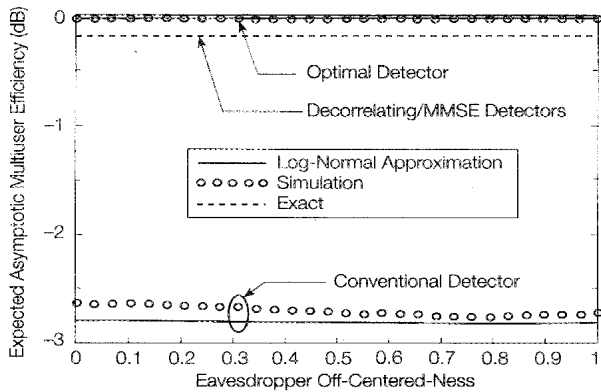


Fig. 15 - Asymptotic multiuser efficiency for various detection strategies in log-normal shadowing with standard deviation 10 dB (two uniformly-distributed users with cross-correlation $\rho = 0.2$).

distance path loss model, the received power ratio with shadowing is also log-normal with zero mean and standard deviation $4\sigma_S^2 + \sigma_R^2$ dB.

Fig. 15 depicts the AME of various eavesdropper detection strategies for a two-user power-controlled system subject to log-normal shadowing with standard deviation 10 dB, where the users are uniformly and independently located and exhibit signal cross-correlation $\rho = 0.2$. Comparing with Fig. 9, which was computed without consideration to shadowing effects, it is apparent that performance sensitivity to eavesdropper off-centered-ness is reduced by the effect of shadowing, an expected product of the location-independent contribution to received power variance represented by shadowing. In addition, the performance loss incurred by use of conventional detection is increased in the presence of shadowing. Fig. 16 depicts BER performance curves for the same system with a background SNR level of 10 dB. The effect of shadowing in comparison to Fig. 13 is seen to flatten the performance curves, representative of a decreased sensitivity of eavesdropper performance to location, a result of the dominant effect of shadowing on received power variance.

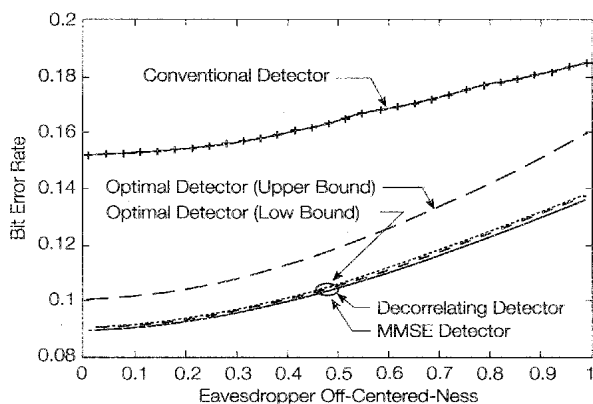


Fig. 16 - Bit Error Rate for various detection strategies in log-normal shadowing with standard deviation = 10 dB (two uniformly-distributed users with cross-correlation $\rho = 0.2$, SNR = 10 dB).

5. CONCLUSIONS

We have demonstrated that the off-center eavesdropper is susceptible to the near-far problem in cellular power-controlled CDMA systems. In fact, we have shown that power control actually increases near-far susceptibility by increasing the potential range of received powers from independent and uniformly located users, and by increasing the variance of received powers resulting from log-normal shadowing in systems wherein the power control at the base station performs shadowing compensation. We conclude, therefore, that to the benefits of power control we can add the property of robustification against eavesdropping.

The distribution of received power from an active user with uniformly random location using a log-distance path loss model was developed for cells with circular and linear geometries, leading to an analysis of eavesdropper outage probabilities for a fixed desired user in cells with different loads. The exact distribution of received power ratio for a linear cell with two uniformly random and independently situated users was given, and a log-normal model shown to provide a good approximation. Eavesdropper outage probabilities for two randomly located users were computed as well.

In order to improve performance in light of the demonstrated near-far problem, several multiuser detection strategies exhibiting various levels of computational complexity were considered for use by an eavesdropper in a cellular CDMA system. A performance comparison for a two-user circular cell was carried through using a log-normal approximation to the distribution of received power ratio under the criterion of asymptotic multiuser efficiency, with results supported by simulation. A comparison of bit error rates for different detectors was also performed via simulation of the users' locations using exact expressions for bit error rate. These comparisons demonstrated the potential for a significant improvement in eavesdropper performance through the use of non-conventional detection techniques.

Finally, we incorporated log-normal shadowing effects into the eavesdropper performance analysis. A performance comparison for a two-user system subject to both log-distance path loss and shadowing also demonstrated a significant performance improvement using multiuser detection strategies.

Manuscript received on December 18, 1997.

REFERENCES

- [1] S. Ariyavisitakul, L. F. Chang: *Signal and interference statistics of a CDMA system with feedback power control*. "IEEE Trans. Commun.", Vol. 41, No. 11, Nov. 1993, p. 1626-1634.
- [2] S. Ariyavisitakul: *Signal and interference statistics of a CDMA system with feedback power control - part II*. "IEEE Trans. Commun.", Vol. 42, No. 2/3/4, Feb/Mar/Apr. 1994, p. 597-605.

- [3] S. Verdú: *Multiuser detection*. Cambridge University Press, New York, 1998.
- [4] R. Lupas, S. Verdú: *Linear multiuser detectors for synchronous code-division multiple-access channels*. "IEEE Trans. Inform. Theory", Vol. IT-35, No. 1, Jan. 1989, p. 123-136.
- [5] Z. Xie, R.T. Short, C.K. Rushforth: *A family of suboptimum detectors for coherent multiuser communications*. "IEEE J. Select. Areas Commun.", Vol. 8, No. 4, May 1990, p. 683-690.
- [6] A. Abdulrahman, D. D. Falconer, A. U. Sheikh: *Decision feedback equalization for CDMA in indoor wireless communications*. "IEEE J. Select. Areas Commun.", Vol. 12, No. 4, May 1994, p. 698-706.
- [7] U. Madhow, M. Honig: *MMSE interference suppression for direct-sequence spread-spectrum CDMA*. "IEEE Trans. Commun.", Vol. COM-42, No. 12, Dec. 1994, p. 3178-3188.
- [8] S. L. Miller: *An adaptive direct-sequence code-division multiple-access receiver for multiuser interference rejection*. "IEEE Trans. Commun.", Vol. COM-43, No. 2/3/4, Feb/Mar/Apr. 1995, p. 1556-1565.
- [9] P. B. Rapajic, B. S. Vucetic: *Adaptive receiver structures for asynchronous CDMA systems*. "IEEE J. Select. Areas Commun.", Vol. 12, No. 4, May 1994, p. 685-697.
- [10] M. Honig, U. Madhow, S. Verdú: *Blind multiuser detection*. "IEEE Trans. Inform. Theory", Vol. IT-41, No. 4, July 1995, p. 944-960.
- [11] X. Wang, H. V. Poor: *Blind equalization and multiuser detection in dispersive CDMA channels*. "IEEE Trans. Commun.", Vol. 46, No. 1, Jan. 1998, p. 91-103.
- [12] X. Wang, H. V. Poor: *Blind multiuser detection: a subspace approach*. To appear in "IEEE Trans. Inform. Theory", Mar. 1998.
- [13] T. S. Rappaport: *Wireless communication: principles and practice*. Prentice Hall PTR, 1996.